Tunable TE-Mode Resonators based on Ferroelectric AlScN Thin Films for RF Applications

Mingyo Park
School of Electrical and Computer Engineering
Georgia Institute of Technology
Atlanta, GA, USA
m.park@gatech.edu

Azadeh Ansari
School of Electrical and Computer Engineering
Georgia Institute of Technology
Atlanta, GA, USA
azadeh.ansari@ece.gatech.edu

***Abstract*—This work presents the characterization of ferroelectric Aluminum Scandium Nitride (AlScN) thin films for multi-frequency high-order overtone mode resonators used in radio frequency (RF) filtering applications. Three types of AlScN-based thickness-extensional (TE) mode resonators are co-fabricated on the same silicon-on-insulator (SOI) platform, 1) High-overtone Bulk Acoustic Resonator (HBAR), 2) Composite Film Bulk Acoustic Resonator (C-FBAR), and 3) Thin Film Bulk Acoustic Resonator (FBAR). We report on the experimental results and analysis of acoustic characteristics and ferroelectric behavior in the $Al_{0.7}Sc_{0.3}N$-based thickness extensional (TE) mode resonators with these different substrate configurations. We observed the effect of thin-film stress on coercive field and evaluated the loss mechanism depending on a substrate layer underneath the sandwiched piezoelectric structure.**

Keywords— Ferroelectric; Acoustic resonators; FBAR; Composite FBAR; HBAR; Aluminum Scandium Nitride(AlScN);

I. Introduction

The advanced wireless radio frequency (RF) systems have increased the demand for high-performance RF modules to fulfill the ever-increasing frequency bands [1]. Muti-frequency tunable filters would play a key role with various radio protocols operating at different frequencies [1], [2]. Recently, we reported on thin-film bulk acoustic resonator (FBAR) [3] and composite FBAR (C-FBAR) [5] based on ferroelectric Aluminum Scandium Nitride ($Al_{1-x}Sc_xN$) thin films, promising candidates for multi-frequency tunable filters [4]. Ferroelectric-based thin film devices have gained attention due to the frequency tuning and intrinsic polarization switching behaviors [3]. Moreover, adding a substrate layer underneath the FBAR resonant stack, when optimized in thickness and acoustic velocity, can enable multi-mode resonance with boosted quality factor (Q) and device robustness [5]. This can prevent thin-film stress issues found in conventional FBARs [5].

In order to design low-loss, multi-frequency, and tunable RF components by targeting high overtone modes with AlScN-on-substrate, it is required to characterize 1) the frequency dependency on both tunability and the film dielectric loss (tanδ) [6] and 2) substrate effects on thin films, such as undesired parasitic capacitance or increased resistivity caused by the passive layer underneath the resonant stack. The high conductivity accumulation in substrate surface causes charge defects in the interface between the piezo-stack and substrate, which challenges the electrical isolation of integrated devices [7] with the loss degradation. Therefore, the loss mechanism originating from the substrate needs to be studied since such degradation eventually determines the overall Q [7].

In this work, we demonstrate $Al_{0.7}Sc_{0.3}N$-based thickness-extensional (TE) resonators employed on different substrate configurations to investigate various acoustic properties and the loss mechanism caused by the substrate effects on the films. We took advantage of the improved DC tunability due to the enhanced piezoelectric response by using Sc/(Al+Sc) >27% [8]. We observed box-like ferroelectric hysteresis behavior on a $Mo/Al_{0.7}Sc_{0.3}N/Mo/Si$ resonant stack. We evaluated the tanδ and the total Q of HBAR (with Si) and FBAR (without Si) to analyze the loss mechanism based on the substrate existence.

II. Three Types of $AL_{0.7}SC.3N$ based TE Mode Resonators

The sequential fabrication process steps are demonstrated in Fig.1. The Mo (0.1μm)/$Al_{0.7}Sc_{0.3}N$ (0.9μm)/Mo (0.1μm) stack is sputter-deposited on an Si (3.55μm)/SiO_2 (0.1μm)/Si (650μm) SOI substrate (Fig.1(a)). The Three types of AlScN TE mode resonators —HBAR(d), C-FBAR(e), and FBAR (f)— are co-fabricated with different substrate configurations. Fig.1(g) illustrates the measured frequency responses (FR) of HBAR, C-FBAR, and FBAR. Compared to stand-alone FBAR, C-FBAR and HBAR offer muti-resonance modes with a comb-like spectrum (with spacing Δf) induced by the Si layer.

III. Experimental Result

Fig.2 shows the measured hysteresis behavior of the $Al_{0.7}Sc_{0.3}N$ ferroelectric film-based HBAR and C-FBAR with box-like P-E loops. The coercive field is decreased from 3MV/cm to 2.5MV/cm, and the polarization range is reduced from ±50 to ±35μC/cm^2 due to applied stress in thin film with varied Si thickness [9]. Fig.3. shows the C-V curve and tanδ of the FBAR and HBAR using bias voltage at -20 to 20V at the input frequency of 50kHz. The calculated C-V modulation of FBAR and HBAR is 413ppm/V to 372ppm/V, respectively. The measured tanδ of HBAR has a higher loss than the FBAR since HBAR loss is increased by resistivity due to accumulated charges at the interface between the piezo-layer and substrate [7], [10], as shown in the smith chart FR in Fig.4(a). The measured Q_{max} based on the FR of HBAR (=680) is lower than FBAR (=1150) with the same trend as shown in the tanδ.

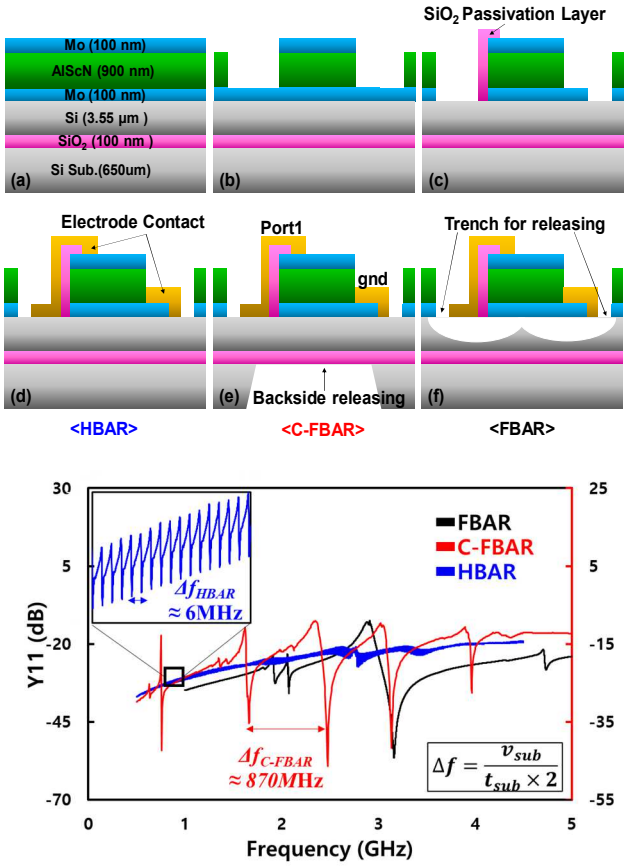

Fig. 1 The fabrication process of the AlScN Acoustic resonators: (a) starting wafer cross-section schematic; (b) top electrode patterning and $Al_{0.7}Sc_{0.3}N$ etching; (c) bottom electrode patterning and SiO_2 isolation layer deposition; (d) Ti/Au deposition for electrode contacts of HBAR; (e) backside DRIE of Si handle layer to release C-FBARs; (f) front side release of the FBARs from Si device layer. (g) The measured frequency responses of (d)HBAR, (e) C-FBAR, and (f) FBAR.

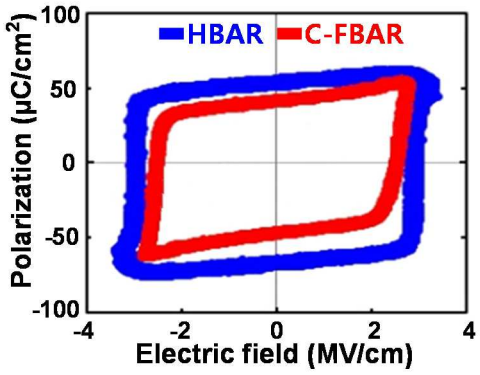

Fig. 2 The hysteresis P-E loop of the $Al_{0.7}Sc_{0.3}N$ based HBAR (blue) and C-FBAR(red) taken at an input frequency of 1kHz. C-FBAR shows reduced coercive field due to increased film stress by reducing a substrate thickness [9].

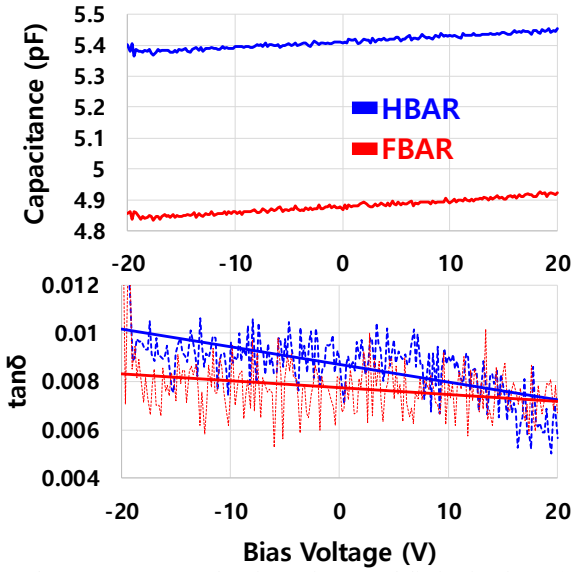

Fig. 3. The measurement results of capacitance and dissipation factor (tan(δ)) for the HBAR and FBAR at 50kHz.

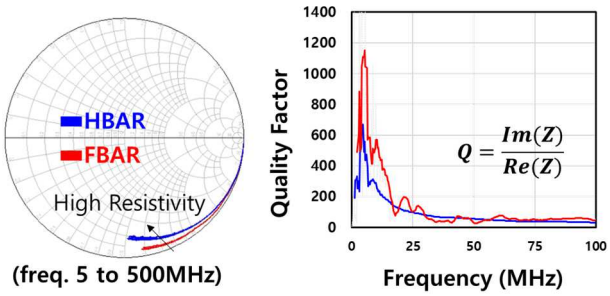

Fig. 4 The measured (a) S11 frequency responses in smith chart, and (b) the calculated device quality factor of HBAR and FBAR.

References

[1] W. Tuttlebee, *Software Defined Radio: Enabling Technologies*. 2002.

[2] A. Tombak *et al.*, "Voltage-controlled RF filters employing thin-film barium-strontium-titanate tunable capacitors," *IEEE Trans. Microw. Theory Tech.*, vol. 51, no. 2 I, pp. 462–467, 2003

[3] J. Wang *et al*, "Ferroelectric Aluminum Scandium Nitride Thin Film Bulk Acoustic Resonators with Polarization-Dependent Operating States," *PSS - Rapid Res. Lett.*, vol. 15, no. 5, pp. 1–6, 2021.

[4] S. S. Gevorgian *et al*, "Introduction," in *Tuneable Film Bulk Acoustic Wave Resonators*, London, U.K.: Springer, 2013, pp. 1–15.

[5] M. Park, J. Wang, and A. Ansari, "High-Overtone Thin Film Ferroelectric AlScN-on-Silicon Composite Resonators," *IEEE Electron Device Lett.*, vol. 42, no. 6, pp. 911–914, 2021

[6] J. S. Fu *et al*, "A linearity improvement technique for thin-film barium strontium titanate capacitors," *IEEE MTT-S Int. Microw. Symp. Dig.*, pp. 560–563, 2006, doi: 10.1109/MWSYM.2006.249654.

[7] S. Gevorgian and A. Vorobiev, "Substrates, Varactors and Passive Components," in *Ferroelectrics in Microwave Devices, Circuits and Systems*, 2009, pp. 115–173.

[8] E. Defaÿ *et al*, "Tunability of aluminum nitride acoustic resonators: A phenomenological approach," *IEEE Trans. Ultrason. Ferroelectr. Freq. Control*, vol. 58, no. 12, pp. 2516–2520, 2011.

[9] N. Setter *et al.*, "Ferroelectric thin films: Review of materials, properties, and applications," *J. Appl. Phys.*, vol. 100, no. 5, 2006.

[10] M. Rack *et al*, "Modeling of Semiconductor Substrates for RF Applications: Parti-Static and Dynamic Physics of Carriers and Traps," *IEEE Trans. Electron Devices*, vol. 68, no. 9, pp. 4598–4605, 2021.